Inhibition of curli assembly and *Escherichia coli* biofilm formation by the human systemic amyloid precursor transthyretin

Neha Jain[a], Jörgen Ådén[b], Kanna Nagamatsu[a], Margery L. Evans[a], Xinyi Li[c], Brennan McMichael[a], Magdalena I. Ivanova[d,e], Fredrik Almqvist[b], Joel N. Buxbaum[c,1], and Matthew R. Chapman[a,1]

[a]Department of Molecular, Cellular, and Developmental Biology, University of Michigan, Ann Arbor, MI 48109-1048; [b]Department of Chemistry, Umeå University, 901 87 Umeå, Sweden; [c]Department of Molecular Medicine, The Scripps Research Institute, La Jolla, CA 92037; [d]Department of Neurology, University of Michigan, Ann Arbor, MI 48109-1048; and [e]Program of Biophysics, University of Michigan, Ann Arbor, MI 48109-1048

Edited by Ralph R. Isberg, Howard Hughes Medical Institute/Tufts University School of Medicine, Boston, MA, and approved October 10, 2017 (received for review May 28, 2017)

During biofilm formation, *Escherichia coli* and other Enterobacteriaceae produce an extracellular matrix consisting of curli amyloid fibers and cellulose. The precursor of curli fibers is the amyloidogenic protein CsgA. The human systemic amyloid precursor protein transthyretin (TTR) is known to inhibit amyloid-β (Aβ) aggregation in vitro and suppress the Alzheimer's-like phenotypes in a transgenic mouse model of Aβ deposition. We hypothesized that TTR might have broad antiamyloid activity because the biophysical properties of amyloids are largely conserved across species and kingdoms. Here, we report that both human WT tetrameric TTR (WT-TTR) and its engineered nontetramer-forming monomer (M-TTR, F87M/L110M) inhibit CsgA amyloid formation in vitro, with M-TTR being the more efficient inhibitor. Preincubation of WT-TTR with small molecules that occupy the T4 binding site eliminated the inhibitory capacity of the tetramer; however, they did not significantly compromise the ability of M-TTR to inhibit CsgA amyloidogenesis. TTR also inhibited amyloid-dependent biofilm formation in two different bacterial species with no apparent bactericidal or bacteriostatic effects. These discoveries suggest that TTR is an effective antibiofilm agent that could potentiate antibiotic efficacy in infections associated with significant biofilm formation.

amyloids | CsgA | transthyretin | biofilms | curli

Microbial biofilms allow colony survival and dispersal. However, in that context they represent a threat to the environment and human health by fouling surfaces and allowing infections to persist despite seemingly adequate antibiotic therapy (1–3). Enteric bacteria, like *Escherichia coli*, produce an extracellular functional amyloid known as curli that is a critical component of the surface-associated biofilm matrix (4, 5). Amyloids are ordered, extremely stable, fibrillar structures of ∼10 nm in diameter (6) that bind the dyes Congo red and Thioflavin T (ThT) and have a dominant parallel or antiparallel β-sheet structure (7). In vivo amyloid deposits are generally extracellular and are insoluble under physiological conditions of pH and ionic strength. While amyloid formation in humans is generally associated with disease (8–12), many microorganisms make amyloidogenic proteins, which have "functional" roles in the biology of the microbial cell (13, 14).

Curli production is dependent on the curli-specific gene (*csg*) operons, which encode the major structural components and accessory proteins (15–18). The major subunit of the curli amyloid fiber, CsgA, is synthesized in the cytoplasm and transported to the cell surface as an unfolded protein, where it assembles to form extracellular amyloid polymers upon interaction with the CsgB nucleator protein (19, 20). Although CsgA amyloid formation in vivo is dependent on CsgB, in vitro CsgA can self-assemble into amyloid fibers in its absence (21). The export of Csg proteins to the outer surface is guided by the accessory proteins, CsgG, CsgE, and CsgF (22–25). Recently, the periplasmic protein CsgC has been recognized as a potent and specific inhibitor of CsgA amyloid formation in vitro and keeps CsgA soluble in vivo (26). Thus, bacteria have evolved a well-coordinated molecular machinery to prevent intracellular aggregation. However, they allow export of amyloid precursors to the outer surface of the membrane where the precursors can assemble and serve as the scaffold around which cellulose and extracellular DNA can assemble extracellular matrix and functional biofilm (5, 14).

The curli inhibitor, CsgC, is structurally similar to the human amyloid precursor transthyretin (TTR) (Fig. S1). TTR and CsgC are both stably folded, β-sheet–rich proteins (27–30). TTR is a 55-kDa homotetramer synthesized primarily in the liver, choroid plexus, and retina (27). It transports thyroxine (T4) and retinol binding protein charged with retinol in plasma and cerebrospinal fluid (31, 32). As a human systemic amyloidosis precursor, TTR tetramers dissociate to release monomers, which rapidly misfold, and aggregates to form fibrillar tissue deposits responsible for familial amyloidotic polyneuropathy, familial amyloidotic cardiomyopathy, and senile systemic amyloidosis (33, 34). Despite its association with disease, TTR has been found to inhibit amyloid formation and subsequent toxicity by other known amyloidogenic proteins, such as amyloid-β (Aβ), a model amyloidogenic

Significance

Functional amyloids, like curli, contribute to biofilm development by uropathogenic *Escherichia coli* and other Gram-negative bacteria. Biofilms allow pathogens to subvert immune defenses and antibiotic treatments. Therefore, strategies to interrupt bacterial biofilm formation are urgently required. Here, we discovered that human transthyretin potently inhibits biofilm formation by *E. coli* and *Bacillus subtilis*. Transthyretin inhibits biofilm formation by preventing curli proteins from adopting the functional amyloid state that supports biofilm development. To our knowledge, this report of amyloid-dependent biofilm inhibition by a human protein with no significant bactericidal or bacteriostatic activity is unique. The observations indicate that a conformational relationship relevant to a set of specific protein–protein interactions, independent of primary sequence, can be functional across biological kingdoms.

Author contributions: N.J., J.N.B., and M.R.C. designed research; N.J., J.Å., K.N., M.L.E., and B.M. performed research; N.J., J.Å., K.N., M.L.E., X.L., M.I.I., and F.A. contributed new reagents/analytic tools; N.J., J.Å., M.I.I., F.A., J.N.B., and M.R.C. analyzed data; and N.J., J.N.B., and M.R.C. wrote the paper.

The authors declare no conflict of interest.

This article is a PNAS Direct Submission.

[1]To whom correspondence may be addressed. Email: jbux@scripps.edu or chapmanm@umich.edu.

This article contains supporting information online at www.pnas.org/lookup/suppl/doi:10.1073/pnas.1708805114/-/DCSupplemental.

bacterial peptide (HypF-N), and human islet amyloid polypeptide in vitro, abrogating cytotoxicity and fibril formation in a fashion similar to the ATP-independent chaperones αB-crystalline and clusterin (35–40). While the engineered nontetrameric form of TTR (M-TTR; F87M/L110M) (41) has greater intrinsic fiber-forming propensity, it is also a more effective inhibitor of amyloid formation by other precursors in vitro than the WT tetramer (WT-TTR).

The established antiamyloid behavior of TTR and the structural resemblance of the monomer to CsgC prompted us to examine the ability of TTR to inhibit CsgA amyloid formation in vitro and CsgA-dependent biofilm formation in vivo. In the present study, we find that both forms of TTR (M-TTR and WT-TTR) can inhibit bacterial amyloid formation in vitro. In addition, both inhibited curli-dependent pellicle-biofilm formation without any bactericidal or bacteriostatic effects. We propose that this property of TTR has potential use in strategies designed to combat biofilm formation in clinical and environmental settings.

Results

TTRs Inhibit Conversion of Soluble CsgA into Amyloid Fibrils. To investigate whether TTR could modulate CsgA amyloid assembly in vitro, we monitored fibril formation by ThT fluorescence, as previously described (17). CsgA polymerization displayed a typical sigmoidal response with an increase in ThT fluorescence after a lag time of 2.5 ± 0.5 h, reaching a plateau after 8 h (Fig. 1 *A* and *B*). Addition of WT-TTR to freshly purified CsgA at a molar ratio 1:1 increased the lag phase to 4 h (Fig. 1*A*), suggesting that WT-TTR interferes with the early nucleation and elongation stages of amyloidogenesis. When added to soluble CsgA at the same ratio (1:1), M-TTR abolished CsgA fibril formation (Fig. 1*B*). The inhibitory activity was concentration-dependent for both WT-TTR and M-TTR. However, M-TTR was found to be more effective, as it inhibited CsgA amyloid formation at substoichiometric ratios (Fig. 1 *A* and *B* and Fig. S2). To determine the specificity of CsgA amyloid inhibition by TTR, we studied CsgA fibrillation in the presence of BSA, which is similar in size, charge distribution, and structural stability to the TTR tetramer and human lysozyme, which is of similar size but has a significantly different pI than M-TTR. No change in the extent or kinetics of CsgA aggregation was observed in the presence of either BSA or lysozyme (Fig. 1*C*), indicating that inhibition of CsgA amyloid formation by TTR was not a result of nonspecific protein–protein interactions.

M-TTR Sequesters CsgA into Dead-End Oligomers/Aggregates. To better assess how TTR arrested CsgA amyloid formation, we carried out transmission electron microscopy (TEM) of CsgA incubated with TTR. TEM revealed clear distinctions between the species generated by CsgA in the presence of the different forms of TTR (Fig. 2). Neither preparation showed detectable oligomers or aggregates at time 0 (Fig. 2 *A*–*C*). After 15 h of incubation, CsgA formed infinite stretches of self-assembled ribbon-like amyloid fibers (Fig. 2*D*). In contrast, CsgA incubated with WT-TTR for 15 h generated fewer and thinner fibers (Fig. 2*E*), which upon longer incubation (~36 h) formed typical CsgA fibers. More strikingly, when incubated with M-TTR for 15 h, CsgA formed predominantly amorphous aggregates consistent with their failure to bind ThT (Fig. 2*F*). Extending the incubation period up to 48 h failed to reveal any evidence for conversion/maturation of the amorphous aggregates into fibrils (Fig. S3).

To better understand the morphological features of the aggregates, we performed atomic force microscopy (AFM). CsgA alone formed typical fibers after incubation for 15 h (Fig. 3*A*), whereas CsgA incubated with M-TTR revealed a uniform distribution of spherical aggregates (Fig. 3*B*), suggesting that M-TTR directs CsgA into structures, which are incompetent for amyloid fiber formation. To gain further insight into how M-TTR affected the structural transitions of CsgA over time, and how the two proteins interact, we performed NMR analysis. Freshly prepared CsgA was incubated in an NMR tube at 25 °C for 76 h to monitor the structural transitions during amyloid formation. After 76 h, there was a dramatic decrease in 1D spectra intensity (Fig. 3*C*), consistent with CsgA monomers being converted to larger molecular species no longer detectable in the spectrum. The same experiment was performed in the presence of unlabeled M-TTR (1:1 ratio to the ^{15}N-labeled CsgA). At 76 h, the samples displayed little or no decrease in signal intensity, suggesting that M-TTR prevents the loss of signal due to amyloid formation in vitro (Fig. 3*D*). M-TTR makes only a minimal and distinct contribution to the CsgA+M-TTR spectrum (Fig. 3*D*). Thus, the combined results from the TEM, AFM, and NMR studies suggest that M-TTR directs CsgA into off-pathway oligomers/aggregates, which are incompetent for fiber formation.

M-TTR, but Not WT-TTR, Inhibits Seeded Aggregation by CsgA. The substoichiometric molar ratios of M-TTR required for CsgA amyloid inhibition led us to speculate that M-TTR may interact with multiple conformational species of CsgA present in solution. It is believed that the increased rate of amyloid fibril formation after the initial aggregates are formed is related to secondary nucleation at multiple sites along the primary fibrils. This secondary nucleation can be assessed in assays where sonicated preformed fibers—or seeds—can bypass the usual lag phase in CsgA polymerization (11, 42, 43). We monitored the antiamyloid activity of M-TTR and WT-TTR in the absence and presence of exogenously added 2% (by weight) seeds to CsgA under amyloid-forming conditions. CsgA amyloid assembly is accelerated by the addition of CsgA seeds (Fig. 4*A*). The addition

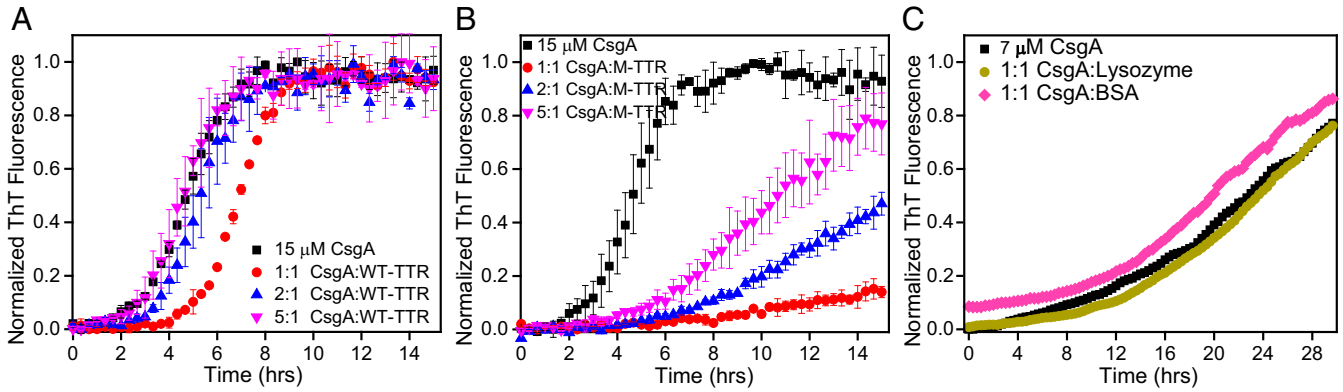

Fig. 1. Transthyretin inhibits CsgA amyloid formation in vitro. Purified CsgA was incubated with substoichiometric concentrations of (*A*) WT-TTR, (*B*) M-TTR, and (C) BSA and human lysozyme (Lyz). Aggregation kinetics were monitored by ThT fluorescence.

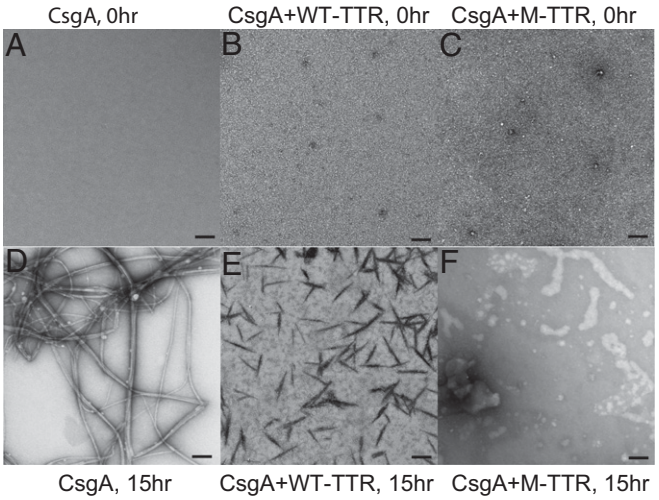

Fig. 2. Microscopy images documenting fibers and aggregates. Representative TEM images taken at zero time point showed no aggregation in (*A*) 15 μM CsgA, (*B*) 1:1 CsgA: WT-TTR, and (*C*) 1:1 CsgA: M-TTR. Images taken after 15 h of incubation depicted (*D*) CsgA fibers, (*E*) thin proto-fibril like structures when CsgA incubated with WT-TTR at 1:1 molar ratio, and (*F*) unstructured amorphous aggregates when CsgA incubated with M-TTR at 1:1 molar ratio. (Scale bars, 100 nm.)

of WT-TTR to CsgA in a molar ratio of 1:1 failed to influence the kinetics of seeded CsgA aggregation (Fig. 4*B*). However, the addition of M-TTR at the same ratio substantially inhibited the accelerating effect of CsgA seeding (Fig. 4*C*), suggesting an effect of M-TTR on secondary nucleation, via an interaction with a molecular species other than the CsgA monomer, to interrupt fibril formation.

The TTR T4 Binding-Site Is Involved in WT-TTR Inhibitory Activity. Given the differences in inhibitory activity of WT-TTR and M-TTR, we hypothesized that the different TTR's have distinct modes of inhibition of fibril formation. To test this hypothesis we examined the effects of several molecules that have been shown to occupy the T4 binding site of the TTR tetramer. We compared the effect of tafamidis, a drug demonstrated to stabilize the TTR tetramer on the capacities of WT-TTR and M-TTR (which does not form a T4-binding site) to inhibit CsgA fibrillogenesis (44). WT-TTR and M-TTR were incubated with tafamidis overnight at 37 °C before addition to the CsgA fibrillation reaction. The inhibitory effect of WT-TTR on CsgA aggregation was completely abolished at a molar ratio of 1:1 in the presence of tafamidis (Fig. 5*A*), whereas the M-TTR inhibitory activity remained unaltered (Fig. S4*A*). The results suggest that the T4 binding-site needs to be unoccupied for tetrameric TTR to inhibit CsgA amyloid formation. However, it is also possible that the tetrameric TTR (WT-TTR) dissociates to yield monomeric TTR, which actually inhibits fibril formation and that tafamidis, by stabilizing the tetramer, blocks monomer release. This possibility was explored by testing the capacity of a highly stable human TTR tetramer mutant (T119M) to inhibit CsgA aggregation (45) (Fig. 5*A*). Its inhibitory capacity was comparable to that of tetrameric WT-TTR. The inhibitory capacity of TTR T119M was unaffected by preincubation with tafamidis because the amino acid substitution at position 119 abrogates tafamidis binding (46). To further explore whether the tafamidis effect was based on occupation of the T4 binding site per se, or stabilization of the homotetramer, we performed a similar experiment with two other small molecules (resveratrol: a plant polyphenol, and A2: an engineered stilbene) that are known to occupy the T4 binding pocket in both WT-TTR and the T119M TTR mutant (47, 48). These have the additional advantage that both are nonfluorescent in an aqueous environment but fluoresce at characteristic wavelengths when bound in the T4 pocket of tetrameric TTR (Fig. S4 *B* and *C*). When incubated with either resveratrol or A2, WT-TTR and T119M lost their capacity to delay CsgA polymerization (Fig. 5 *B* and *C*), while M-TTR did not (Fig. S4*A*). Thus, it is likely that the antiamyloidogenic action of the human TTR tetramer (WT-TTR) with CsgA is mediated primarily through the T4 binding pocket and does not require tetramer dissociation and monomer release. However, it is possible that other regions in TTR may also participate in the inhibition of CsgA fibrillogenesis.

TTR Inhibits the Conversion of CsgA and CsgB Variants into Amyloid Fibrils. CsgA contains five imperfect repeating units (R1–R5) that contribute to CsgA amyloid formation. Deletion of segments R1 (ΔR1), R3 (ΔR3), and R5 (ΔR5) did not significantly alter CsgA amyloid assembly and each variant retained the capacity for fibril formation in vitro (18, 49). The ability of the different TTR conformers to affect amyloid formation by the various CsgA deletion mutants was also assessed. M-TTR completely inhibited amyloid assembly by each variant, whereas WT-TTR only delayed the appearance of fibers by the CsgA ΔR1, CsgA ΔR3, and CsgA ΔR5 (Fig. S5 *A*–*C*). Hence, their effects on the subunits were similar to those seen with full-length CsgA. The results suggest either that TTR has multiple interactive sites on CsgA or that each mutant presents a similar TTR-interactive conformation to the environment.

CsgA polymerization into curli amyloid fibers in vivo is dependent on the minor curli subunit CsgB, which serves to template curli amyloid formation on the cell surface (20). CsgB shares ~30% sequence identity with CsgA and forms amyloid fibrils that can seed CsgA amyloid formation (21). We tested the ability of TTR conformers to inhibit CsgB fibril formation using a truncated variant of CsgB ($CsgB_{trunc}$), which has a slower rate of amyloid formation than full-length CsgB and has a detectable lag phase. M-TTR inhibited $CsgB_{trunc}$ from assembling into

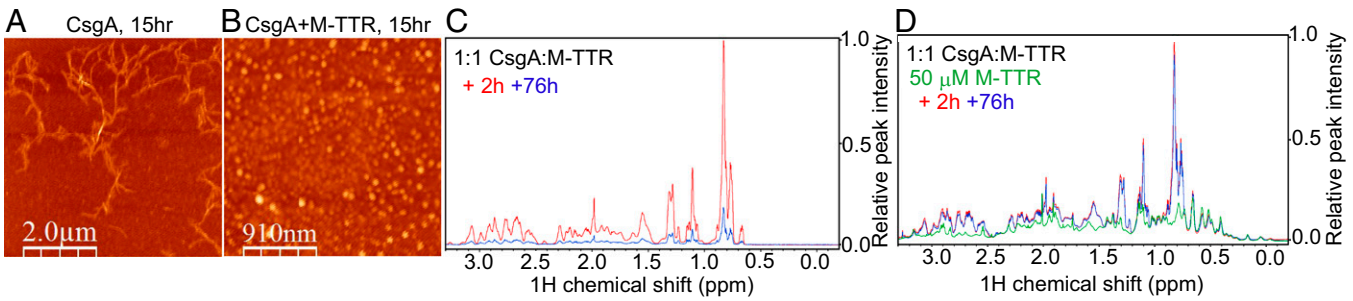

Fig. 3. Structural transitions of CsgA in presence of transthyretin. AFM images taken after 15 h showed (*A*) CsgA (15 μM) fibers and (*B*) spherical oligomers when CsgA incubated with M-TTR at 1:1 molar ratio. (*C*) Relative peak intensities of 1D NMR data showing major signal decays in the aliphatic region of CsgA after 76 h of incubation as the protein turns into amyloid fibers. (*D*) The experiment was repeated in the presence of 1:1 CsgA: M-TTR and 50 μM M-TTR alone.

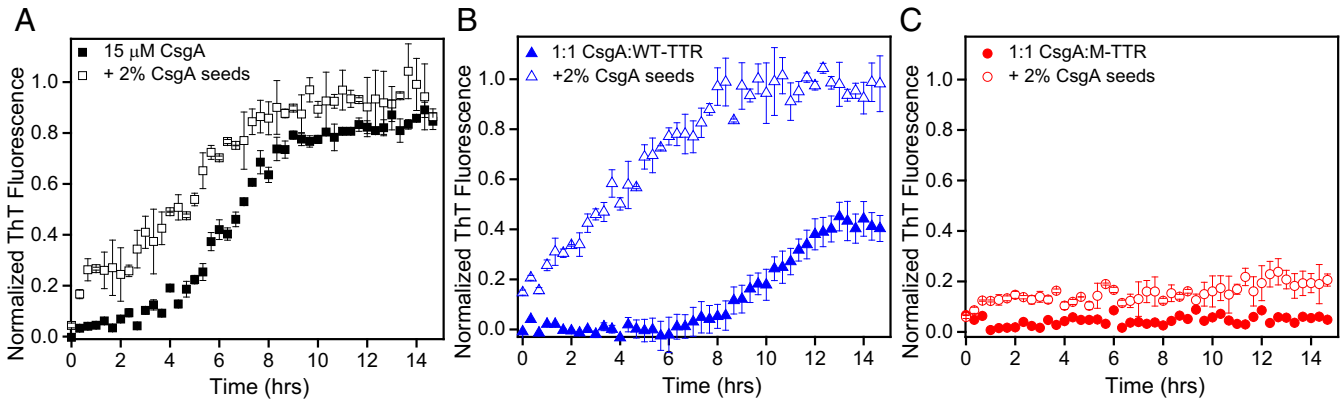

Fig. 4. Effect of transthyretin on seeded CsgA aggregation. Polymerization of CsgA in the presence of 2% (wt/vol) preformed and sonicated CsgA fibrils (CsgA seeds) prepared as described in *Materials and Methods*. (*A*) CsgA seeds accelerated CsgA polymerization. (*B*) CsgA seeds accelerated CsgA polymerization in presence of WT-TTR. (*C*) CsgA seeded polymerization inhibited by M-TTR.

amyloid, whereas WT-TTR did not significantly alter $CsgB_{trunc}$ fibril formation (Fig. S5*D*) at a molar ratio of 1:1. The results demonstrate that among Csg-related amyloidogenic proteins the antiamyloid activity of both WT-TTR and M-TTR is not sequence-specific.

TTRs Did Not Dissociate Preformed CsgA Fibers. Some chaperones are capable of disaggregating protein aggregates (50, 51). To determine if TTR could disaggregate mature CsgA amyloid fibers, we incubated 2-d-old CsgA amyloid fibers with and without either WT-TTR or M-TTR. No significant change in ThT fluorescence was observed in the presence of either form of TTR (Fig. S6*A*). After 3 d, the TEM images of CsgA plus TTR (WT-TTR and M-TTR) revealed a mesh of fibers that were indistinguishable from the CsgA only fibers with no evidence of disaggregation (Fig. S6 *B–D*). These results suggest that neither WT nor M-TTR has intrinsic disaggregase activity for mature CsgA fibers.

TTRs Abolish Curli-Dependent Pellicle Biofilm Formation of Uropathogenic *E. coli* UTI89. The distinct differences in CsgA amyloid assembly in the absence and presence of TTR prompted us to ask whether the effect was biologically relevant. In other words, could TTR interfere with amyloid-dependent pellicle biofilm formation in *E. coli*? For pellicle assays, we used UTI89, an *E. coli* originally isolated from a patient with an acute urinary tract infection (52, 53). To test the antibiofilm activity of the two forms of TTR, we added increasing concentrations of WT-TTR or M-TTR to the *E. coli* UTI89 cultures (Fig. 6) and monitored the development of biofilm at 26 °C for 48 h.

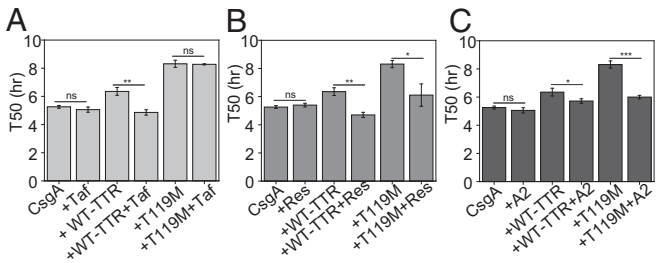

Fig. 5. Effect of occupied T4 binding site on CsgA amyloid inhibition. CsgA polymerization expressed as T50 in presence of tetrameric TTR (WT-TTR and T119M mutant) incubated without and with small molecules that bind in the T4 site: (*A*) with tafamidis (taf), (*B*) with resveratrol (res), (*C*) with A2. Presence of small molecules in T4 site abolished the inhibitory activity of WT-TTR and T119M mutant. *ns*, not significant, $*P < 0.03$, $**P < 0.002$, $***P < 0.0002$.

UTI89 formed wrinkled pellicle biofilms at the air–liquid interface when incubated in media (Fig. 6*A*, *Top*). In contrast, pellicle formation was markedly diminished when either WT-TTR (Fig. 6*A*, *Middle*) or M-TTR (Fig. 6*A*, *Bottom*) were added at the beginning of the incubation. WT-TTR reduced biofilm biomass by 40%, while M-TTR was much more potent, achieving an 80% reduction compared with the untreated cells (Fig. 6*B*). TEM analysis of UTI89 grown under pellicle-inducing conditions revealed a mesh of curli fibers that held the cells together in large clumps (Fig. 6*C* and Fig. S7*A*). UTI89 grown under the same conditions, but treated with WT-TTR, had fewer visible fibers (Fig. 6*D* and Fig. S7*B*). However, UTI89 grown under pellicle-inducing conditions in the presence of M-TTR had almost no curli-like fibers with the cells evenly dispersed around the grid (Fig. 6*E* and Fig. S7*C*). The growth curves of UTI89 cells in the absence or presence of TTR were nearly identical, suggesting that the effects on biofilm formation were not related to TTR having bacteriostatic or bactericidal activity (Fig. 6*F*).

Because biofilm formation is common to most bacterial species, we investigated if the TTR inhibition of biofilm formation was species-specific. We tested the capacity of M-TTR to inhibit biofilm formation by *Bacillus subtilis*, a Gram-positive bacterium that forms amyloid-dependent floating pellicle biofilms at the air–liquid interface dependent on the amyloid scaffold formed by the TasA protein (54). The cells grown in media alone developed a pellicle in 36 h (Fig. S8*A*), whereas the cells with exogenously added M-TTR did not show any pellicle formation (Fig. S8*B*). As with *E. coli*, the growth of *B. subtilis* was unaltered in the presence of M-TTR (Fig. S8*C*). These results indicate that TTR (specifically M-TTR) can inhibit amyloid-dependent biofilm formation by more than one bacterial species.

Discussion

The effects of the two forms of TTR on fibril formation by CsgA, a functional amyloid protein that comprises the major component of *E. coli* biofilm, were similar to those seen with Aβ fibrillogenesis, suggesting that the effects were on the process of amyloidogenesis independent of the primary sequence or species of origin of the amyloid-forming protein. Our results from ThT fluorescence and NMR analysis show that the conversion of soluble CsgA to amyloid fibrils can be inhibited by the WT-TTR tetramer but more efficiently by an engineered M-TTR that does not form tetramers (Fig. 1). The TEM analyses indicate that WT-TTR delays the appearance of CsgA amyloid fibers, while M-TTR does not inhibit CsgA oligomerization per se; rather, it prevents the formation of the higher-order CsgA protofibrillar and fibrillar structures that ultimately comprise the biofilm scaffold (Fig. 2). The failure to see shifted resonances in the NMR studies could be consistent with a transient interaction, a

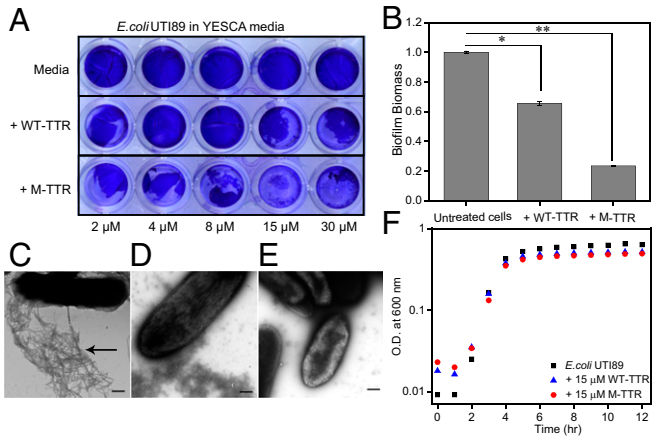

Fig. 6. Transthyretin suppressed pellicle-biofilm formation in *E. coli* UTI89. (*A*) Concentration-dependent effect of WT-TTR and M-TTR on biofilm formation in *E. coli* UTI89 grown in YESCA media at 26 °C for 48 h under quiescent conditions. *E. coli* UTI89 in media (*Top*), +WT-TTR (*Middle*), and +M-TTR (*Bottom*). (*B*) Biofilm biomass quantification in untreated cells and cells with exogenously added WT-TTR and M-TTR. $*P = 0.001$ and $**P < 0.0001$. Representative TEM images of (*C*) *E. coli* UTI89 cells, (*D*) *E. coli* UTI89 cells with 15 μM WT-TTR, and (*E*) *E. coli* UTI89 cells with 15 μM M-TTR. (Scale bars, 300 nm.) The arrow indicates network of curli fibers. (*F*) Growth curves of *E. coli* UTI89 in absence and presence of WT-TTR and M-TTR.

global molecular effect with minimal interaction with specific amino acids or, most likely, simply technical in that the soluble aggregates formed in the presence of M-TTR are too large to be adequately interrogated by NMR (Fig. 3). This observation is consistent with the AFM images showing CsgA oligomers/aggregates in the presence of M-TTR, which are amorphous and likely to be off the amyloid pathway (Fig. 3).

The likelihood that the mechanisms of inhibition of aggregation may be fundamentally different for M-TTR and WT-TTR is also supported by the observation that only M-TTR can inhibit both seeded and unseeded CsgA amyloid assembly (Fig. 4). Additional evidence for distinct modes of inhibition are the effects on fibrillogenesis of three different small molecules known to block the T4 binding site in WT-TTR. Tafamidis, resveratrol, and A2 had no apparent effect on the inhibition of CsgA fibril formation by M-TTR, but abolished the inhibitory activity of WT-TTR (Fig. 5 and Fig. S4*A*). These results are similar to the inhibition of Aβ fibril formation by M-TTR, which was also unaffected by tafamidis (37). Thus, it appears that an available T4 binding site is required for WT-TTR to inhibit amyloid formation by CsgA. Because M-TTR has no T4 binding site, it must have a different mechanism of interaction.

In vitro analyses of the TTR–Aβ interaction from several laboratories have demonstrated that the engineered M-TTR is also a much more potent inhibitor of Aβ fibril formation than the functional tetramer (37, 55). It has been proposed that because of its inherent capacity to oligomerize rapidly, M-TTR forms nonfibrillar oligomers that behave as substoichiometric polyvalent binders of Aβ oligomers, while binding by the tetramer is stoichiometric (35, 37). Based on the observed increased antiamyloid activity of M-TTR compared with the tetrameric WT-TTR, it was proposed that tetramer dissociation is required to release the monomers, which are the active species for fibril inhibition. The fact that the inhibition experiments are performed under conditions in which there is little dissociation of TTR tetramers makes this unlikely. Furthermore, the fact that highly stable TTR tetramers, such as TTR T119M, which do not dissociate to any degree under physiologic conditions, can still inhibit fibrillogenesis indicates that tetramer dissociation is not required for inhibition of CsgA amyloidogenesis (Fig. 5).

The potential biological importance of the in vitro demonstration of the anti-CsgA amyloid activity of TTR was realized in the experiments in which TTR was shown to inhibit amyloid-dependent biofilm formation (Fig. 6). Because WT-TTR does not inhibit the aggregation of CsgB, yet is capable of inhibiting biofilm formation, it is likely that its effect is via its interaction with CsgA. However, since M-TTR inhibits fibrillogenesis by both CsgA and CsgB, we cannot definitively state whether its biofilm inhibitory capacity is via an interaction with CsgA, CsgB, or both. Importantly, neither WT-TTR nor M-TTR exhibited cytotoxicity, allowing us to conclude that biofilm inhibition is due to suppression of amyloid formation rather than an effect on bacterial growth or metabolism (Fig. 6*F*).

Bacterial biofilm formation compromises efforts to eradicate infections with antibiotics, particularly in contexts where the colonies form on inanimate bio-compatible surfaces, such as indwelling catheters and orthopedic implants (56). Numerous antimicrobial peptides and small molecules have been designed to prevent biofilm formation or disperse preexisting biofilms in the clinical as well as industrial contexts (24, 57, 58). Most peptides designed for antibiofilm activity are known to also have antimicrobial activity. Our results demonstrate that M-TTR completely abolished amyloid-dependent biofilm formation by two different bacterial species, with WT-TTR being less potent than M-TTR, and suggests that M-TTR might be used as an antibiofilm factor on inert surfaces (Fig. 6). Neither of the proteins (WT-TTR and M-TTR) had any apparent effect on bacterial growth, indicating that the mechanism was mediated by its action on biofilm formation rather than via an effect on bacterial metabolism or physiology, and hence, should not interfere with the actions of antibiotics that are dependent on interfering with replication or metabolism.

To our knowledge, this is a unique report in which the antiamyloid property of a human protein (TTR) has been exploited in bacterial systems to inhibit amyloids and biofilms without having significant antimicrobial activity. The LL-37 protein, while behaving as a natural antibiofilm factor for many bacterial species (e.g., *Pseudomonas aeruginosa*, *E. coli*, and *Staphylococcus aureus*) also modulates the host immune response (59–61). Truncated fragments of LL-37 and another cationic peptide 1037 have been shown to inhibit biofilms from *P. aeruginosa*, *E. coli*, *S. aureus*, *Burkholderia cenocepacia*, and *Listeria monocytogenes* (62–64). Both LL-37 and peptide 1037 are known to disrupt lipid membranes (antimicrobial activity) and alter gene expression (antibiofilm activity) (64). Hence, the mode of action of LL-37 and other cationic peptides is likely to be distinct from that of TTR.

To summarize, we have demonstrated that the amyloidogenic protein TTR may behave in a chaperone-like manner to inhibit bacterial curli fibrillogenesis and biofilm formation. Our results suggest that TTR may be used to enhance treatment or prophylaxis of infections characterized by prominent biofilm formation.

Materials and Methods

See also *SI Materials and Methods*. The effect of TTR variants on kinetics of CsgA, CsgA mutants, and $CsgB_{trunc}$ amyloid formation was monitored in 96-well black flat-bottom plates using automated microtiter plate reader (Tecan Infinite M200). Freshly purified CsgA, CsgA mutants, and $CsgB_{trunc}$ were diluted in 50 mM KPi (pH 7.3) to a final protein concentration of 15 μM. The samples were incubated at 25 °C with 20 μM ThT under quiescent conditions. The ThT fluorescence intensity was recorded after every 20 min with linear shaking for 3 s before the readings (excitation: 438 nm; emission: 495 nm; cut-off: 475 nm). Since TTR itself is amyloidogenic, we verified that TTR variants used in the present study did not show appreciable ThT binding under the experimental conditions. For the seeding experiments, CsgA fibers (2-d-old) were sonicated with two 15-s bursts on ice to prepare the seeds. The final values in all ThT experiments are reported as normalized from 0 to 1 using Origin Pro V 9.0 software. All ThT assays were performed in triplicate with at least three biological replicates. Results of fibril-forming experiments are expressed as an average of three biological replicates with SE and are compared as T50, which is the time required for the ThT signal to reach half its maximal fluorescence.

ACKNOWLEDGMENTS. We thank M.R.C. laboratory members for critically reading the manuscript; Pennelope Blakely and the Microsciopy and Image Analysis Laboratory core at University of Michigan for help with transmission electron microscopy images; and the Mukhopadhyay laboratory at the Indian Institute of Science Education and Research, Mohali, India for access and help with atomic force microscopy images. This work was financially supported by Grant R01-GM118651 (to M.R.C.); an Mcubed grant (to M.R.C. and M.I.I.); the Protein Folding Disease Initiative (M.I.I.); the Swedish Research Council; the Knut and Alice Wallenberg Foundation; the Göran Gustafsson Foundation; and the Swedish Foundation for Strategic Research (F.A.). K.N. was partly supported by a subaward from Washington University to University of Michigan from Grant R01-AI099099.

1. Costerton JW, Stewart PS, Greenberg EP (1999) Bacterial biofilms: A common cause of persistent infections. *Science* 284:1318–1322.
2. Hall-Stoodley L, Costerton JW, Stoodley P (2004) Bacterial biofilms: From the natural environment to infectious diseases. *Nat Rev Microbiol* 2:95–108.
3. Fux CA, Costerton JW, Stewart PS, Stoodley P (2005) Survival strategies of infectious biofilms. *Trends Microbiol* 13:34–40.
4. Chapman MR, et al. (2002) Role of *Escherichia coli* curli operons in directing amyloid fiber formation. *Science* 295:851–855.
5. Hufnagel DA, DePas WH, Chapman MR (2015) The biology of the Escherichia coli extracellular matrix. *Microbiol Spectr* 3:MB-0014-2014.
6. Nelson R, et al. (2005) Structure of the cross-beta spine of amyloid-like fibrils. *Nature* 435:773–778.
7. Li H, et al. (2009) Amyloids and protein aggregation—Analytical methods. *Encyclopedia of Analytical Chemistry*, ed Mayers RA (John Wiley, Hoboken, NJ), pp 1–23.
8. Chiti F, Dobson CM (2006) Protein misfolding, functional amyloid, and human disease. *Annu Rev Biochem* 75:333–366.
9. Fowler DM, et al. (2006) Functional amyloid formation within mammalian tissue. *PLoS Biol* 4:e6.
10. Maji SK, et al. (2009) Functional amyloids as natural storage of peptide hormones in pituitary secretory granules. *Science* 325:328–332.
11. Knowles TPJ, Vendruscolo M, Dobson CM (2014) The amyloid state and its association with protein misfolding diseases. *Nat Rev Mol Cell Biol* 15:384–396.
12. Dobson CM (2017) The amyloid phenomenon and its links with human disease. *Cold Spring Harb Perspect Biol* 9:a023648.
13. Fowler DM, Koulov AV, Balch WE, Kelly JW (2007) Functional amyloid—From bacteria to humans. *Trends Biochem Sci* 32:217–224.
14. Hufnagel DA, Tükel C, Chapman MR (2013) Disease to dirt: The biology of microbial amyloids. *PLoS Pathog* 9:e1003740.
15. Hammar M, Arnqvist A, Bian Z, Olsen A, Normark S (1995) Expression of two csg operons is required for production of fibronectin- and congo red-binding curli polymers in *Escherichia coli* K-12. *Mol Microbiol* 18:661–670.
16. Barnhart MM, Chapman MR (2006) Curli biogenesis and function. *Annu Rev Microbiol* 60:131–147.
17. Wang X, Smith DR, Jones JW, Chapman MR (2007) In vitro polymerization of a functional *Escherichia coli* amyloid protein. *J Biol Chem* 282:3713–3719.
18. Wang X, Hammer ND, Chapman MR (2008) The molecular basis of functional bacterial amyloid polymerization and nucleation. *J Biol Chem* 283:21530–21539.
19. Hammar M, Bian Z, Normark S (1996) Nucleator-dependent intercellular assembly of adhesive curli organelles in *Escherichia coli*. *Proc Natl Acad Sci USA* 93:6562–6566.
20. Hammer ND, Schmidt JC, Chapman MR (2007) The curli nucleator protein, CsgB, contains an amyloidogenic domain that directs CsgA polymerization. *Proc Natl Acad Sci USA* 104:12494–12499.
21. Hammer ND, et al. (2012) The C-terminal repeating units of CsgB direct bacterial functional amyloid nucleation. *J Mol Biol* 422:376–389.
22. Nenninger AA, Robinson LS, Hultgren SJ (2009) Localized and efficient curli nucleation requires the chaperone-like amyloid assembly protein CsgF. *Proc Natl Acad Sci USA* 106:900–905.
23. Nenninger AA, et al. (2011) CsgE is a curli secretion specificity factor that prevents amyloid fibre aggregation. *Mol Microbiol* 81:486–499.
24. Andersson EK, et al. (2013) Modulation of curli assembly and pellicle biofilm formation by chemical and protein chaperones. *Chem Biol* 20:1245–1254.
25. Goyal P, et al. (2014) Structural and mechanistic insights into the bacterial amyloid secretion channel CsgG. *Nature* 516:250–253.
26. Evans ML, et al. (2015) The bacterial curli system possesses a potent and selective inhibitor of amyloid formation. *Mol Cell* 57:445–455.
27. Blake CC, Geisow MJ, Oatley SJ, Rérat B, Rérat C (1978) Structure of prealbumin: Secondary, tertiary and quaternary interactions determined by Fourier refinement at 1.8 A. *J Mol Biol* 121:339–356.
28. Hamilton JA, Benson MD (2001) Transthyretin: A review from a structural perspective. *Cell Mol Life Sci* 58:1491–1521.
29. Salgado PS, Taylor JD, Cota E, Matthews SJ (2011) Extending the usability of the phasing power of diselenide bonds: SeCys SAD phasing of CsgC using a non-auxotrophic strain. *Acta Crystallogr D Biol Crystallogr* 67:8–13.
30. Taylor JD, et al. (2016) Electrostatically-guided inhibition of curli amyloid nucleation by the CsgC-like family of chaperones. *Sci Rep* 6:24656.
31. Nilsson SF, Rask L, Peterson PA (1975) Studies on thyroid hormone-binding proteins. II. Binding of thyroid hormones, retinol-binding protein, and fluorescent probes to prealbumin and effects of thyroxine on prealbumin subunit self association. *J Biol Chem* 250:8554–8563.
32. Monaco HL, Rizzi M, Coda A (1995) Structure of a complex of two plasma proteins: Transthyretin and retinol-binding protein. *Science* 268:1039–1041.
33. Westermark P, Sletten K, Johansson B, Cornwell GG, 3rd (1990) Fibril in senile systemic amyloidosis is derived from normal transthyretin. *Proc Natl Acad Sci USA* 87:2843–2845.
34. Lashuel HA, Lai Z, Kelly JW (1998) Characterization of the transthyretin acid denaturation pathways by analytical ultracentrifugation: Implications for wild-type, V30M, and L55P amyloid fibril formation. *Biochemistry* 37:17851–17864.
35. Liu L, Murphy RM (2006) Kinetics of inhibition of beta-amyloid aggregation by transthyretin. *Biochemistry* 45:15702–15709.
36. Li X, Masliah E, Reixach N, Buxbaum JN (2011) Neuronal production of transthyretin in human and murine Alzheimer's disease: Is it protective? *J Neurosci* 31:12483–12490.
37. Li X, et al. (2013) Mechanisms of transthyretin inhibition of β-amyloid aggregation in vitro. *J Neurosci* 33:19423–19433.
38. Yang DT, Joshi G, Cho PY, Johnson JA, Murphy RM (2013) Transthyretin as both a sensor and a scavenger of β-amyloid oligomers. *Biochemistry* 52:2849–2861.
39. Cascella R, et al. (2013) Transthyretin suppresses the toxicity of oligomers formed by misfolded proteins in vitro. *Biochim Biophys Acta* 1832:2302–2314.
40. Mangrolia P, Yang DT, Murphy RM (2016) Transthyretin variants with improved inhibition of β-amyloid aggregation. *Protein Eng Des Sel* 29:209–218.
41. Jiang X, et al. (2001) An engineered transthyretin monomer that is non-amyloidogenic, unless it is partially denatured. *Biochemistry* 40:11442–11452.
42. Cohen SIA, et al. (2011) Nucleated polymerization with secondary pathways. I. Time evolution of the principal moments. *J Chem Phys* 135:065105.
43. Zhou Y, et al. (2012) Promiscuous cross-seeding between bacterial amyloids promotes interspecies biofilms. *J Biol Chem* 287:35092–35103.
44. Bulawa CE, et al. (2012) Tafamidis, a potent and selective transthyretin kinetic stabilizer that inhibits the amyloid cascade. *Proc Natl Acad Sci USA* 109:9629–9634.
45. Quintas A, Saraiva MJ, Brito RM (1997) The amyloidogenic potential of transthyretin variants correlates with their tendency to aggregate in solution. *FEBS Lett* 418:297–300.
46. Li X, Song Y, Sanders CR, Buxbaum JN (2016) Transthyretin suppresses amyloid-β secretion by interfering with processing of the amyloid-β protein precursor. *J Alzheimers Dis* 52:1263–1275.
47. Reixach N, et al. (2008) Human-murine transthyretin heterotetramers are kinetically stable and non-amyloidogenic. A lesson in the generation of transgenic models of diseases involving oligomeric proteins. *J Biol Chem* 283:2098–2107.
48. Choi S, Ong DST, Kelly JW (2010) A stilbene that binds selectively to transthyretin in cells and remains dark until it undergoes a chemoselective reaction to create a bright blue fluorescent conjugate. *J Am Chem Soc* 132:16043–16051.
49. Wang X, Chapman MR (2008) Sequence determinants of bacterial amyloid formation. *J Mol Biol* 380:570–580.
50. Mogk A, Bukau B (2004) Molecular chaperones: Structure of a protein disaggregase. *Curr Biol* 14:R78–R80.
51. Månsson C, et al. (2014) Interaction of the molecular chaperone DNAJB6 with growing amyloid-beta 42 (Aβ42) aggregates leads to sub-stoichiometric inhibition of amyloid formation. *J Biol Chem* 289:31066–31076.
52. Cegelski L, et al. (2009) Small-molecule inhibitors target *Escherichia coli* amyloid biogenesis and biofilm formation. *Nat Chem Biol* 5:913–919.
53. Zhou Y, Smith DR, Hufnagel DA, Chapman MR (2013) Experimental manipulation of the microbial functional amyloid called curli. *Methods Mol Biol* 966:53–75.
54. Branda SS, Chu F, Kearns DB, Losick R, Kolter R (2006) A major protein component of the *Bacillus subtilis* biofilm matrix. *Mol Microbiol* 59:1229–1238.
55. Du J, Murphy RM (2010) Characterization of the interaction of β-amyloid with transthyretin monomers and tetramers. *Biochemistry* 49:8276–8289.
56. Römling U, Balsalobre C (2012) Biofilm infections, their resilience to therapy and innovative treatment strategies. *J Intern Med* 272:541–561.
57. Worthington RJ, Richards JJ, Melander C (2012) Small molecule control of bacterial biofilms. *Org Biomol Chem* 10:7457–7474.
58. Joseph R, et al. (2016) Cationic pillararenes potently inhibit biofilm formation without affecting bacterial growth and viability. *J Am Chem Soc* 138:754–757.
59. Scott MG, Davidson DJ, Gold MR, Bowdish D, Hancock REW (2002) The human antimicrobial peptide LL-37 is a multifunctional modulator of innate immune responses. *J Immunol* 169:3883–3891.
60. Dürr UHN, Sudheendra US, Ramamoorthy A (2006) LL-37, the only human member of the cathelicidin family of antimicrobial peptides. *Biochim Biophys Acta* 1758: 1408–1425.
61. Overhage J, et al. (2008) Human host defense peptide LL-37 prevents bacterial biofilm formation. *Infect Immun* 76:4176–4182.
62. de la Fuente-Núñez C, et al. (2012) Inhibition of bacterial biofilm formation and swarming motility by a small synthetic cationic peptide. *Antimicrob Agents Chemother* 56:2696–2704.
63. Nagant C, et al. (2012) Identification of peptides derived from the human antimicrobial peptide LL-37 active against biofilms formed by *Pseudomonas aeruginosa* using a library of truncated fragments. *Antimicrob Agents Chemother* 56:5698–5708.
64. Aka ST (2015) Killing efficacy and anti-biofilm activity of synthetic human cationic antimicrobial peptide cathelicidin hCAP-18/LL37 against urinary tract pathogens. *J Microbiol Infect Dis* 5:15–20.
65. Horcas I, et al. (2007) WSXM: aA software for scanning probe microscopy and a tool for nanotechnology. *Rev Sci Instrum* 78:013705.